



# Production of lipid-based fuels and chemicals from microalgae: An integrated experimental and model-based optimization study



M. Bekirogullari <sup>a,b</sup>, I.S. Fragkopoulos <sup>a</sup>, J.K. Pittman <sup>c</sup>, C. Theodoropoulos <sup>a,b,\*</sup>

<sup>a</sup> School of Chemical Engineering and Analytical Science, University of Manchester, Manchester M13 9PL, UK

<sup>b</sup> Biochemical and Bioprocess Engineering Group, University of Manchester, Manchester M13 9PL, UK

<sup>c</sup> Faculty of Life Sciences, University of Manchester, Manchester M13 9PT, UK

## ARTICLE INFO

### Article history:

Received 6 August 2016

Received in revised form 14 October 2016

Accepted 21 December 2016

Available online xxx

### Keywords:

*Chlamydomonas reinhardtii*

Biofuels

Kinetic modelling

Microalgal oil

Nitrogen starvation

Acetate utilization

## ABSTRACT

Cultivation of microalgae is a promising long-term, sustainable candidate for biomass and oil for the production of fuel, food, nutraceuticals and other added-value products. Attention has been drawn to the use of computational and experimental validation studies aiming at the optimisation and the control of microalgal oil productivity either through the improvement of the growth mechanism or through the application of metabolic engineering methods to microalgae. Optimisation of such a system can be achieved through the evaluation of organic carbon sources, nutrients and water supply, leading to high oil yield. The main objective of this work is to develop a novel integrated experimental and computational approach, utilising a microalgal strain grown at bench-scale, with the aim to systematically identify the conditions that optimise growth and lipid production, in order to ultimately develop a cost-effective process to improve the system economic viability and overall sustainability. To achieve this, a detailed model has been constructed through a multi-parameter quantification methodology taking into account photo-heterotrophic biomass growth. The corresponding growth rate is based on carbon substrate concentration, nitrogen and light availability. The developed model also considers the pH of the medium. Parameter estimation was undertaken using the proposed model in conjunction with an extensive number of experimental data taken at a range of operating conditions. The model was validated and utilised to determine the optimal operating conditions for bench-scale batch lipid oil production.

© 2017 The Authors. Published by Elsevier B.V. This is an open access article under the CC BY license (<http://creativecommons.org/licenses/by/4.0/>).

## 1. Introduction

Fossil fuels provide a non-renewable form of energy that is also finite [12,31]. The use of non-renewable resources negatively impacts on the environment since it leads to the production of harmful greenhouse gas (GHG) emissions [17]. On the contrary, renewable forms of energy sources such as solar and wind energy as well as biomass, are environmentally sustainable [24]. Various biomass sources such as energy crops, animal fat, agricultural residues and fungal or bacterial microbes have been used for the commercial production of biofuels [2]. Biodiesel production is a well-established platform [20], with soybeans, canola oil, palm oil, corn oil, animal fat and waste cooking oil, the most common commercial sources.

Microalgal oil consists of the neutral lipid Triacylglycerol (TAG), which is stored in cytosolic and/or plastidic lipid bodies [18]. The accumulation of such lipid bodies can be enhanced by abiotic stress, including deprivation of nutrients like nitrogen (N) and phosphorus (P), and factors such as light intensity and temperature stress [5,19]. Depending

on the fatty acid characteristics, the oil can be utilised directly or it can be processed into biolubricants, surfactants, nutritional lipids like omega-3 fatty acids, and importantly, into liquid fuels and gas. The use of microalgal oil for biodiesel production has not yet been exploited commercially as the current price of production is still too high compared to fossil fuel diesel. Approximately 60–75% of the total cost of microalgal biodiesel comes from microalgae cultivation, mainly due to the high cost of the carbon source, the fertilizer requirements and the high cultivation facility costs relative to often low oil productivity [22].

However, production of biofuels from microalgal oil bears several advantages both in terms of environmental impact and of sustainability. The main ones are the rapid growth rate of microalgae and high oil productivity per area of land used [26], the reduction of GHG emissions due to the avoidance of fossil fuel combustion and to the use and fixation of available inorganic (CO<sub>2</sub>) and/or waste organic carbon (e.g. waste glycerol), the use of less resources (freshwater and nutrient fertilizer), particularly for marine or wastewater cultivated microalgae [43], and no competition for agricultural land and simple growing needs (light, N, P, potassium (K) and CO<sub>2</sub>) [11,21]. Although microalgal oil has an immense potential in biotechnological applications, metabolic productivity needs to be enhanced to realise economic viability. Strain

\* Corresponding author.

E-mail address: [k.theodoropoulos@manchester.ac.uk](mailto:k.theodoropoulos@manchester.ac.uk) (C. Theodoropoulos).

## Nomenclature

TAG	Triacylglycerol
TAP	Tris-acetate-phosphate
DCW	Dry cell weight
N	Nitrogen
K	Phosphorus
S	Substrate
I	Light intensity
L	Lipid
X	Oil-free biomass
AA	Acetic acid
GA	Glycolic acid
FA	Formic acid
$\mu$	Specific growth rate
$\mu_{max}$	Maximum specific growth rate of biomass
$K_S$	Substrate saturation constant
$K_{IS}$	Substrate inhibition constant
$\mu_X$	Specific growth rate of oil-free biomass
$\mu_{Xmax}$	Maximum specific growth rate of oil-free biomass
$K_{XS}$	Acetate saturation constant
$K_{IXS}$	Acetate inhibition constant
$K_{XN}$	Nitrogen saturation constant
$K_{IXN}$	Nitrogen inhibition constant
$q_L$	Specific growth rate of lipid
$q_{Lmax}$	Maximum specific growth rate of lipid
$K_{LS}$	Acetate saturation constant
$K_{ILS}$	Substrate inhibition constant
$K_{INL}$	Nitrogen inhibition constant
$Y_{X/S}$	Yield coefficient for oil-free biomass production with respect to substrate
$Y_{X/N}$	Yield coefficient for oil-free biomass production with respect to N
$K_H$	pH rate constant
$Y_{L/S}$	Yield coefficient for lipid production with respect to substrate
$K_{XI}$	Light saturation constant
$K_{IXI}$	Light inhibition constant
$K_{LI}$	Light saturation constant
$K_{ILI}$	Light inhibition constant
$\sigma$	Molar extinction coefficient
$k_1$	Parameter of the mathematical model
$K_{GAS}$	Acetate saturation constant
$K_{GAN}$	Nitrogen saturation constant
$K_{IGAN}$	Nitrogen inhibition constant
$k_2$	Parameter of the mathematical model
$K_{FAS}$	Acetate saturation constant
$K_{FAN}$	Nitrogen saturation constant

development by genetic manipulation, mutagenesis or natural selection is one approach that is being actively evaluated [27]. Alternatively, cultivation conditions and metabolic productivity can be optimized based on an integrated combination of mathematical modelling and growth experiments at different scales.

A critical component of sustainable microalgae-derived biofuel productivity is the balance between biomass growth and lipid accumulation, whereby conditions of extreme nutrient starvation that drive substantial cellular lipid accumulation can also significantly inhibit cell growth, and thus net volumetric lipid productivity is low [28]. For this reason, integrated experimental and theoretical studies to model and experimentally validate changes in microalgal metabolism and metabolite yield are an important tool to predict improvements to oil productivity [6,9,35]. The combination of predictive models and experiments allows the development of a framework that will reveal the relationship

between microalgal growth and lipid accumulation which can be used to optimise the balance of biomass and oil productivity from algal strains, in order to ultimately achieve a positive energy balance for a cost-efficient and sustainable scaled-up biodiesel production.

Experimental studies have shown that both microalgae growth and lipid production can be simultaneously and antagonistically affected by two or more nutrients and environmental variables, such as carbon and nutrient concentrations, light intensity, pH and temperature [13,15,19]. However, the majority of the previously developed kinetic models are expressed either as a function of a single nutrient or environmental variable concentration, or as a function of multiple nutrient concentrations. Monod [40] formulated a kinetic model, the so-called Monod model, to analyse the effect of a single nutrient limitation on biomass growth, while the inhibition effects of the nutrient and of other growth parameters were not considered. Andrews [4] constructed an improved version of the Monod model to take into account both the single nutrient limitation and the nutrient inhibition effects, but this study did not take into consideration the inhibition effect of the other growth parameters. Such models have been extensively employed to analyse the effect of a single nutrient. The effect of light was analysed by [29], the effects of one substrate (S) and of pH were investigated by Zhang et al. [50], and the effect of temperature was explored by Bernard and Rémond [10].

The effect of multiple nutrient concentrations can be examined through the use of two other frameworks; the threshold and the multiplicative models [37]. The threshold model considers that the growth is only affected by the growth parameter with the lowest concentration, and therefore, the model takes the form of a single substrate growth model. On the contrary, the multiplicative model takes into account two or more growth parameters that contribute to microalgae growth equally. The threshold model was employed by Spijkerman et al. [46] for the investigation of the effects of substrate and of P concentration, while the multiplicative model was used by Bernard [8] for the analysis of the effects of light intensity and of N concentration. Although the aforementioned models are deemed to be accurate enough to predict the effects of the nutrients, they are not able to predict the simultaneous effects of other factors such as nutrient factors and environmental factors with the same accuracy. Moreover, although the control of microalgal growth and lipid accumulation by multiple factors (such as multiple limiting nutrients) has been investigated on a theoretical basis, the published data are limited and they do not allow conclusions on the kinetic relationship between microalgal growth and lipid accumulation with respect to the concentrations of the limiting nutrients [36].

Here, we present a comprehensive multiplicative kinetic model to describe microalgal growth and the relevant lipid oil production under photo-heterotrophic conditions. The formulated model takes into account the effects of four different growth-promoting resources: acetate (organic carbon substrate for the heterotrophic component of growth), nitrogen, light intensity and pH. The model simulates all of the effects simultaneously and it is capable of predicting the microalgal biomass growth and the lipid accumulation with high accuracy. To efficiently estimate the kinetic parameters that are crucial for accurate system simulations and to validate the developed model, experiments were performed using the well-studied chlorophyte microalgal species *Chlamydomonas reinhardtii* [5,39,45]. We demonstrate that such an integrated experimental-computational framework can be used to provide insights on biomass growth and lipid metabolism, and eventually to enable robust system design and scale-up.

## 2. Materials and methods

### 2.1. Strain and culture conditions

*C. reinhardtii* (CCAP 11/32C) was used here as the experimental microalgal strain, obtained from the Culture Collection of Algae and

Protozoa, UK. The strain was cultivated under photo-heterotrophic conditions in batch cultures [5]. Preculture of the strain was carried out in an environmentally-controlled incubation room at 25 °C, using 250 mL conical flasks containing 150 mL of Tris-acetate-phosphate (TAP) medium [30] (TAP constituents are given in Table S1) on an orbital shaker at 120 rpm for 7–10 days. A 4 ft. long 20 W high power led T8 tube light was used for illumination at a constant  $125 \mu\text{Em}^{-2} \text{s}^{-1}$  light intensity. Once sufficient cell density was reached, an algal inoculum of 1 mL was added to the experimental culture vessels, Small Anaerobic Reactors (SARs, 500 mL), containing 500 mL of modified TAP culture medium (described below) at the same temperature and light conditions as preculturing. The initial cell density of  $0.024 \times 10^6$  cells per mL was identical for all the treatments. The number of cells was determined through the measurement of living cells using a Nexcelom Cellometer T4 (Nexcelom Biosciences). 20  $\mu\text{L}$  of the sample was injected into the cellometer counting chamber and the chamber was then inserted into the apparatus. Once the sample was placed, the following specifications were defined: cell diameter min 1.0  $\mu\text{m}$  and max 1000  $\mu\text{m}$ , roundness 0.30 and contrast enhancement 0.30. Subsequently, the lens was focused in order to count all the cells. The acetate (referred to as substrate, S) and N (as  $\text{NH}_4\text{Cl}$ ) concentration in standard TAP medium was  $1.05 \text{ g L}^{-1}$  and  $0.098 \text{ g L}^{-1}$ , respectively. The TAP culture media was also modified to contain different concentrations of N and acetate in order to induce N or acetate starvation and excess, respectively. Overall, we used six different acetate concentrations: 0  $\text{g L}^{-1}$ , 0.42  $\text{g L}^{-1}$ ,  $1.05 \text{ g L}^{-1}$ , 2.1  $\text{g L}^{-1}$ , 3.15  $\text{g L}^{-1}$  and 4.2  $\text{g L}^{-1}$ ; and seven different N concentrations: 0.0049  $\text{g L}^{-1}$ , 0.0098  $\text{g L}^{-1}$ , 0.049  $\text{g L}^{-1}$ , 0.098  $\text{g L}^{-1}$ , 0.196  $\text{g L}^{-1}$ , 0.98  $\text{g L}^{-1}$  and 1.96  $\text{g L}^{-1}$ . When the concentrations of N were manipulated, the concentration of acetate was kept constant at  $1.05 \text{ g L}^{-1}$ , and when the concentration of acetate were manipulated, the concentration of N was kept constant at  $0.098 \text{ g L}^{-1}$ . The initial pH value of all media was set at pH = 7.

*C. reinhardtii* growth was determined at set time points by biomass measurement. The biomass concentration was measured in terms of dry cell weight (DCW) concentration. DCW was measured by centrifuging 500 mL cultures for 3 min at 3000 g in an Eppendorf Centrifuge 5424. The obtained pellet was then washed with cold distilled water. The washed pellet was centrifuged again for 3 min at 3000 g and weighed on a fine balance (Sartorius - M-Pact AX224, Germany) to determine the wet biomass. Subsequently, the wet biomass was dried overnight at 70 °C to determine the dry biomass weight. The pH of the samples was analysed through the use of a bench type pH meter (Denver UltraBasic Benchtop Meters, USA). The supernatant and the biomass of the samples were kept stored at  $-20 \text{ }^\circ\text{C}$  for quantification of specific metabolites. All data was statistically analysed by one-way ANOVA using Tukey post-hoc test performed using Prism v.6.04 (GraphPad).

## 2.2. Metabolite analysis

### 2.2.1. HPLC analysis of organic acids

The concentrations of organic acids produced and/or consumed were quantified using a High Performance/Pressure Liquid Chromatographer (HPLC) equipped with a Hi-Plex 8  $\mu\text{m}$   $300 \times 7.7 \text{ mm}$  column. Glacial acetic acid (AA) as well as glycolic acid (GA) and formic acid (FA), were included as standards, as these were either growth media substrate (AA) or secreted microalgal by-products of the cultivation as also corroborated by Allen [51]. Sulphuric acid solution (0.05% v/v) was used as a mobile phase. The flow rate of the system was set at  $0.6 \text{ mL min}^{-1}$ , with a pressure value around 45 bars and a temperature of 50 °C, while the detection wavelength was fixed at 210 nm. Filtration through 0.45  $\mu\text{m}$  filter membranes was undertaken for the sample preparation.

### 2.2.2. TOC/TN analyser

The total dissolved N concentration in the growth media was quantified by the use of a Total Organic Carbon/Total Nitrogen analyser (TOC/TN) (TOC-VCSH/TNM-1 Shimadzu). Ammonium chloride ( $\text{NH}_4\text{Cl}$ ), added to the growth media as a nutrient, was used to prepare standard solutions. Three different ammonia ( $\text{NH}_3$ ) sources can be found in TAP media; Ethylenediaminetetraacetic acid (EDTA), Tris-hydroxymethyl-aminomethane (TRIS) and  $\text{NH}_4\text{Cl}$ , which is the form assimilated by the microalgae for biomass growth. In order to quantify the  $\text{NH}_4\text{Cl}$ -originated N, the samples were initially analysed to determine the total N concentration in the media. Then, 100  $\mu\text{L}$  of supernatant first diluted to 1 mL and then mixed with 200  $\mu\text{L}$  of NaOH, and placed into hot water to enable the evaporation of the formed  $\text{NH}_3$  (produced from  $\text{NH}_4\text{Cl}$  through  $\text{NH}_4^+$ ). Finally, the samples were analysed again to determine the total N left in the media. The difference between the two aforementioned measurements equals to the amount of N originated by  $\text{NH}_4\text{Cl}$ .

### 2.2.3. Soxhlet solvent extraction using Soxtec

The lipid concentration was quantified by extracting the lipid using the Soxtec 1043 automated solvent extraction system. The freeze-dried algal biomass was homogenised through a double cycle of liquid  $\text{N}_2$  immersion and pulverisation in a mortar with pestle. The pulverized biomass were then placed into cellulose extraction thimbles and located in the Soxtec unit. The procedure followed to quantify the lipid concentration was boiling for 2 h, rinsing for 40 min and solvent recovery for 20 min. The extraction temperature for the selected solvent, Hexane (ACS spectrophotometric grade,  $\geq 98.5\%$ , Sigma Aldrich, Dorset, UK), was 155 °C [52]. Following the oil extraction performed through the use of Soxtec 1043, the extracted lipids were dried at 100 °C for 1 h, were placed in a vacuum applied desiccator for 1 h, and were weighed to define the lipid concentration gravimetrically.

## 3. Mathematical modelling

### 3.1. Growth kinetics

A number of experiments we conducted in our laboratory, demonstrated that high substrate concentrations act as system inhibitors, and they can significantly reduce the biomass growth and the lipid accumulation rates [7]. To account for substrate inhibition on the transient cell behaviour, a modified Monod equation, the Haldane equation, is extensively applied [4,23,42]:

$$\mu = \mu_{max} \cdot \frac{S}{S + K_s + \frac{S^2}{K_{is}}} \quad \text{Eq. 1}$$

Here  $\mu$  is the specific growth rate,  $\mu_{max}$  the maximum specific growth rate, S the substrate concentration,  $K_s$  the substrate saturation constant, and  $K_{is}$  the substrate inhibition constant.

The depletion of N is known to increase the oil accumulation while it inhibits biomass growth [32,47]. Additionally, light intensity plays a crucial role on microalgae growth and lipid accumulation ([29], [33]). Therefore, the Haldane equation (expressed by Eq. 1) needs to be enhanced to account for the additional effects of N concentration and of light intensity.

Due to the contrasting effect of N on biomass concentration and on lipid accumulation, two different expressions for the N effect as a substrate, similar to the ones presented by Economou et al. [23], were employed here to describe the specific (oil-free) biomass growth and the lipid accumulation rate. Furthermore, the Aiba model [3,49] was taken into consideration for the simulation of the effect of light intensity as a pseudo-substrate.

**Table 1**

Estimated kinetic parameters along with bounds available in the literature.

Parameter	Value (units)	Standard deviation ( $\sigma$ )	Variance to mean ratio $\frac{\sigma^2}{\mu}$	Reference value	Species	Sources
$\mu_{Xmax}$	0.227 h <sup>-1</sup>	0.005	0.021	0.2274	<i>C. reinhardtii</i>	[25]
$K_{XS}$	0.050 g S L <sup>-1</sup>	0.000	0.010	0.028 – 2.295	<i>C. reinhardtii</i>	([15], [50])
$K_{iXS}$	9.923 g S L <sup>-1</sup>	0.130	0.013	0.1557 – 1.76	<i>C. reinhardtii</i>	([50], [16])
$K_{XN}$	0.065 g N L <sup>-1</sup>	0.000	0.007	This study		
$K_{iXN}$	0.500 g N L <sup>-1</sup>	0.001	0.002	This study		
$q_{Lmax}$	0.121 g L g X <sup>-1</sup> h <sup>-1</sup>	0.002	0.013	This study		
$K_{LS}$	6.554 g S L <sup>-1</sup>	0.063	0.010	This study		
$K_{iLS}$	0.110 g S L <sup>-1</sup>	0.002	0.014	This study		
$K_{iNL}$	380.023 g N L <sup>-1</sup>	3.154	0.008	This study		
$Y_{X/S}$	1.470 g X g S <sup>-1</sup>	0.010	0.007	0.7104 – 15.6	<i>C. reinhardtii</i>	([50], [16])
$Y_{X/N}$	6.883 g X g N <sup>-1</sup>	0.183	0.027	18.9		[23]
$K_H$	0.879 L g S <sup>-1</sup>	0.018	0.020	0.8759	<i>C. reinhardtii</i>	[50]
$Y_{L/S}$	0.064 g X g S <sup>-1</sup>	0.005	0.074	0.24	<i>C. protothecoide</i>	[41]
$K_{XI}$	19.519 $\mu$ E m <sup>-2</sup> s <sup>-1</sup>	0.731	0.037	81.38	<i>C. reinhardtii</i>	[25]
$K_{iXI}$	2053.924 $\mu$ E m <sup>-2</sup> s <sup>-1</sup>	33.755	0.016	2500	<i>C. reinhardtii</i>	[25]
$K_{LI}$	15.023 $\mu$ E m <sup>-2</sup> s <sup>-1</sup>	0.461	0.031	This study		
$K_{iLI}$	2152.918 $\mu$ E m <sup>-2</sup> s <sup>-1</sup>	43.688	0.020	This study		
$\sigma$	34.104 g X <sup>-1</sup> L m <sup>-1</sup>	1.221	0.0036	This study		
$k_1$	0.329	0.013	0.040	This study		
$K_{GAS}$	1.456 g S <sup>-1</sup> L <sup>-1</sup>	0.031	0.021	This study		
$K_{GAN}$	12.976 g N <sup>-1</sup> L <sup>-1</sup>	0.189	0.015	This study		
$K_{iGAN}$	2.533 g N <sup>-1</sup> L <sup>-1</sup>	0.040	0.016	This study		
$k_2$	1.4055	0.008	0.006	This study		
$K_{FAS}$	12.976 g S <sup>-1</sup> L <sup>-1</sup>	0.450	0.035	This study		
$K_{FAN}$	2.533 g N <sup>-1</sup> L <sup>-1</sup>	0.059	0.023	This study		

Thus, the specific oil-free biomass growth rate,  $\mu_X$ , is described by a pseudo-triple substrate expression as:

$$\mu_X = \mu_{Xmax} \cdot \frac{S}{S + K_{XS} + \frac{S^2}{K_{iXS}}} \cdot \frac{N}{N + K_{XN} + \frac{N^2}{K_{iXN}}} \cdot \frac{I(l)}{I(l) + K_{XI} + \frac{I(l)^2}{K_{iXI}}} \quad \text{Eq. 2}$$

where  $\mu_{Xmax}$  is the maximum specific growth rate of oil-free biomass on acetate substrate (denoted as substrate onwards), depending on the concentration of nitrogen,  $N$ , and on the local light intensity,  $I(l)$ . Here,  $K_{XS}$ ,  $K_{XN}$  and  $K_{XI}$  are the saturation constants and  $K_{iXS}$ ,  $K_{iXN}$  and  $K_{iXI}$  the inhibition constants for oil-free biomass growth based on substrate, nitrogen concentration and light intensity, respectively. The local light intensity  $I(l)$  is expressed by the Beer-Lambert Equation [6]:

$$I(l) = I_0 \cdot \exp(-\sigma X l) \quad \text{Eq. 3}$$

where  $l$  is the distance between the local position and the external surface of the system,  $I_0$  the incident light intensity,  $\sigma$  the molar extinction coefficient and  $X$  the oil-free biomass concentration [6].

The specific lipid accumulation rate,  $\mu_L$ , is expressed as:

$$\mu_L = q_{Lmax} \cdot \frac{S}{S + K_{LS} + \frac{S^2}{K_{iLS}}} \cdot \frac{K_{iNL}}{N + K_{iNL}} \cdot \frac{I(l)}{I(l) + K_{LI} + \frac{I(l)^2}{K_{iLI}}} \quad \text{Eq. 4}$$

where  $q_{Lmax}$  is the maximum lipid specific growth rate,  $K_{LS}$  and  $K_{LI}$  the saturation constants and  $K_{iLS}$  and  $K_{iLI}$  the inhibition constants for lipid accumulation based on substrate concentration and light intensity, respectively;  $K_{iNL}$  is an inhibition constant used here to describe the lipid production dependent on nitrogen concentration.

### 3.2. Rate equations

The dynamic model developed in this work consists of a set of ordinary differential equations (ODEs) employed for the simultaneous

simulation of microalgal growth, lipid accumulation, substrate and nitrogen consumption, by-product formation and pH change rates.

The microalgal (oil-free biomass) growth rate is expressed as:

$$\frac{dX}{dt} = \mu_X \cdot X \quad \text{Eq. 5}$$

The lipid accumulation (lipid production) rate is described by:

$$\frac{dL}{dt} = \mu_L \cdot X \quad \text{Eq. 6}$$

The substrate consumption rate can be calculated through a mass conservation equation [48]:

$$\frac{dS}{dt} = -\frac{1}{Y_{X/S}} \cdot \frac{dX}{dt} - \frac{1}{Y_{L/S}} \cdot \frac{dL}{dt} \quad \text{Eq. 7}$$

where  $Y_{X/S}$  is the yield coefficient for oil-free biomass production with respect to substrate and  $Y_{L/S}$  is the yield coefficient for lipid production with respect to substrate.

The N consumption rate is given by [50]:

$$\frac{dN}{dt} = -\frac{1}{Y_{X/N}} \cdot \frac{dX}{dt} \quad \text{Eq. 8}$$

where  $Y_{X/N}$  is the yield coefficient for oil-free biomass production with respect to N.

For byproduct formation, only two acids are taken into account in our model: glycolic acid (GA) and formic acid (FA). The formation rates of GA and FA can be described by a multiplicative model, including the effects of acetate and N as follows:

$$\frac{dP_{GA}}{dt} = k_1 \cdot \frac{S}{S + K_{GAS}} \cdot \frac{N}{N + K_{GAN} + \frac{N^2}{K_{iGAN}}} \quad \text{Eq. 9}$$



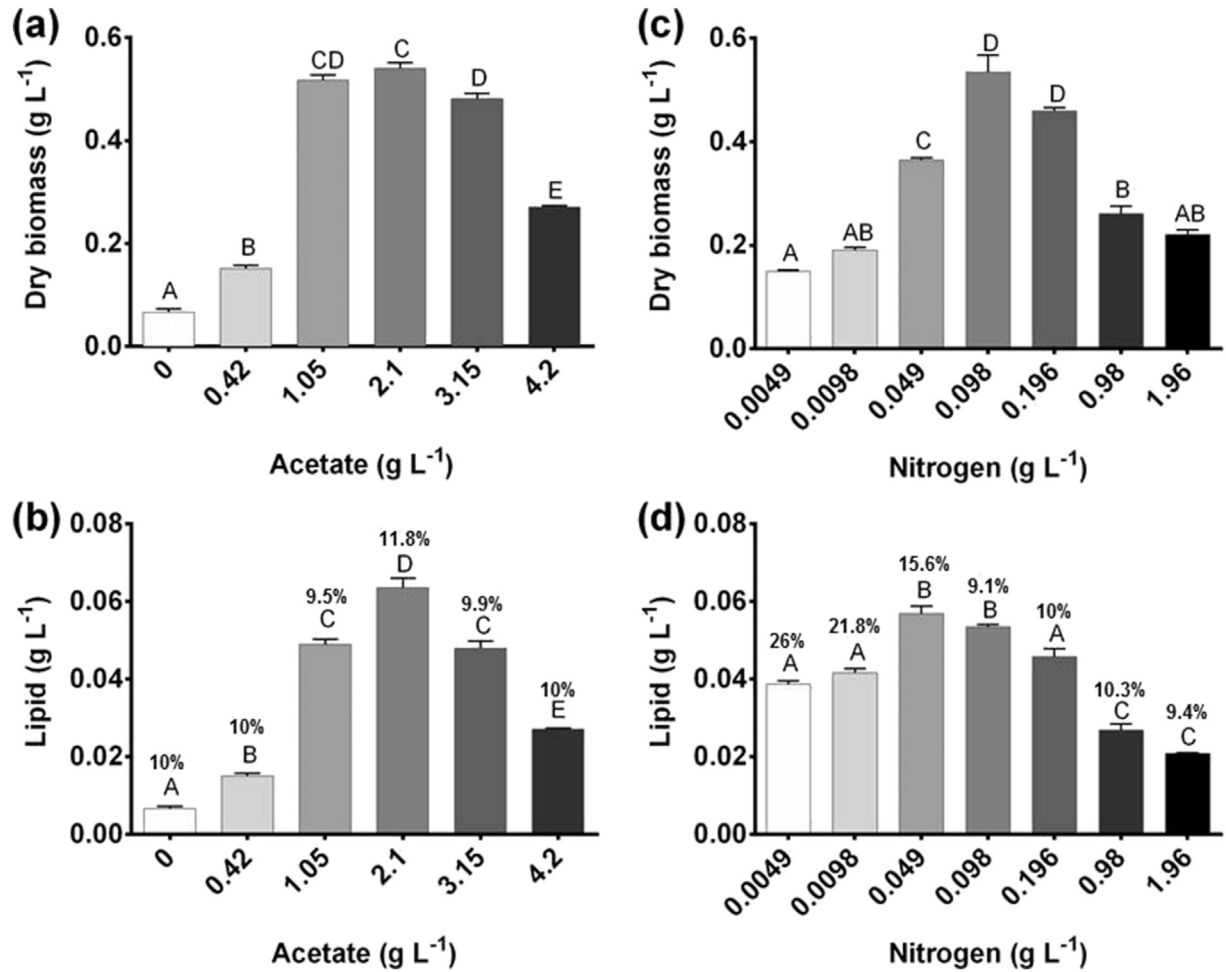


Fig. 1. The effect of carbon substrate (acetate) (a, b) and nutrient (nitrogen, N) (c, d) concentrations on dry weight biomass concentration (a, c) and total lipid concentration (b, d) after photo-heterotrophic growth for 8 d. The starting N concentration for the acetate range treatment experiments was 0.098 g L<sup>-1</sup> and the starting acetate concentration for the N range treatment experiments was 1.05 g L<sup>-1</sup>. All data are mean  $\pm$  SE values of 2–3 biological replicates. Treatments that do not share uppercase letters are significantly different ( $p < 0.05$ ), as determined by one-way ANOVA. The percentage lipid value as a proportion of dry weight biomass is indicated above each bar in panels b and d.

$$\frac{dP_{FA}}{dt} = k_2 \cdot \frac{S}{S + K_{FAS}} \cdot \frac{N}{N + K_{FAN}} \quad \text{Eq. 10}$$

here  $k_1$  and  $k_2$  are kinetic constants,  $K_{GAS}, K_{FAS}$  are substrate and  $K_{GAN}, K_{FAN}$  nitrogen saturation constants;  $K_{IGAN}$  is the nitrogen inhibition constant.

It should be noted here that oxalic acid production was also observed experimentally. The concentration of the oxalic acid (OA) for all the N and acetate treatments remains essentially constant at 0.015 g L<sup>-1</sup> throughout the growth process, which signifies that OA is not a product of the metabolism. Hence its formation was not included in the kinetic model.

The pH change rate of the microalgae cultivation system is proportional to the substrate consumption rate and is expressed by [50]:

$$\frac{dH}{dt} = -K_h \cdot \frac{dS}{dt} \quad \text{Eq. 11}$$

where  $H$  describes the process pH, and  $K_h$  is a constant. Hence our model consists of 7 ODEs, corresponding to 7 state variables describing the dynamic evolution of biomass and lipids as well as that of the substrate, nutrients, pH and byproducts. The model includes 25 parameters, outlined in Table 1 and estimated through the procedure discussed in Section 4.2 below.

### 3.3. Parameter estimation

To the best of our knowledge, this study is the first attempt to model microalgae growth and lipid accumulation by taking into account the simultaneous effect of three growth-promoting resources (N, S, I), and thus, the reaction kinetics for such a system are not available in the literature. For this reason, we undertook a parameter estimation study using the constructed ODE-based system (Eqs. 5 to 11) in conjunction with high fidelity in-house produced experimental data. Two of the experiments discussed above were used (2.1 g L<sup>-1</sup> acetate, 0.098 g L<sup>-1</sup> N –experiment 1–, and 1.05 g L<sup>-1</sup> acetate, 0.049 g L<sup>-1</sup> N –experiment 2–with 1 mg L<sup>-1</sup> biomass, and pH 7, and with starting by-product concentrations all at 0 g L<sup>-1</sup>) The parameter estimation is set up as a non-linear weighted least squares method [48]:

$$Z(kk) = \min \sum_{k=1}^{n_k} \sum_{l=1}^{n_l} \sum_{m=1}^{n_m} W_{k,l,m} \left( C_{k,l,m}^{\text{pred}}(kk) - C_{k,l,m}^{\text{exp}} \right)^2 \quad \text{Eq. 12}$$

Here  $kk$  is the vector of the 25 model parameters,  $n_k$  is the number of experiments ( $n_k = 2$ ),  $n_l$  is the number of state variables ( $n_l = 7$ ),  $n_m$  is the number of experimental measurements in time ( $n_m = 7$ ), and  $W_{k,l,m}$  are the weights used to effectively normalise the computed errors,  $\varepsilon = (C_{k,l,m}^{\text{pred}}(kk) - C_{k,l,m}^{\text{exp}})$ . Here the weights were set to  $W_{k,l,m} = 1/C_{k,l,m}^{\text{exp}}$ , where  $C_{k,l,m}^{\text{pred}}$  are the predicted state variables (computed by Eqs. 5 to 11) and  $C_{k,l,m}^{\text{exp}}$  the experimentally obtained ones.

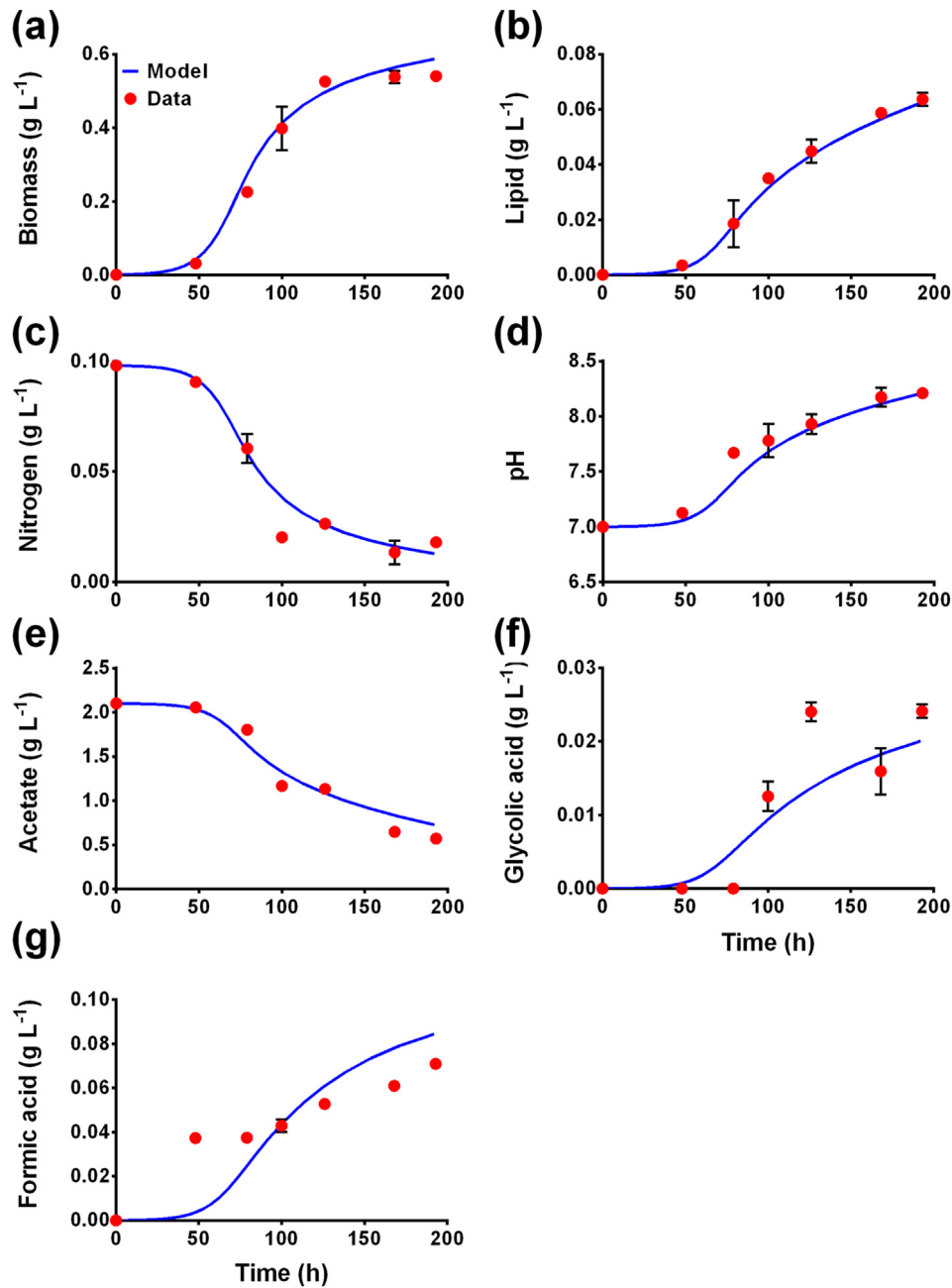


**Fig. 2.** Fitting of model predictions (lines) to experimental data (symbols with error bars) for: (a) biomass, (b) lipid concentration, (c) substrate (acetate) consumption, (d) N consumption, (e) pH change, (f) oxalic acid production, (g) glycolic acid production and (h) formic acid production, using  $2.1 \text{ g L}^{-1}$  acetate and  $0.098 \text{ g L}^{-1}$  N.

The estimation problem was solved using an in-house developed stochastic algorithm, based on Simulated Annealing (SA) [48], with multiple restarts in order to increase the chances of obtaining solutions in the neighbourhood of the global optimum. A refining step using a deterministic method, Sequential Quadratic Programming (SQP) implemented through the “fmincon” function in MATLAB, was subsequently carried out using as initial guess the result from SA.

The initial values of the state variables used in the ODEs were set to the initial concentration values of each experiment. Multiple optimization runs have been used to ensure that the local minima were avoided. The values of the parameters as well as their standard deviation estimated using the above procedure are shown in Table 1. The system dynamics obtained using our model were compared to the experimental results described above, including biomass and lipid growth, pH changes and formation of organic acids, GA and FA. The resulting model shows

very good agreement with the experimental data for all state variables, as can be seen in Fig. 2.

#### 4. Results and discussion

An experimental study was carried out to quantify the effect of varying starting substrate (acetate) and nutrient (N) composition of the growth medium on the system behaviour. A parameter estimation study was then performed using the constructed mathematical model, to compute parameter values that are of crucial importance for accurate system simulations. The model was subsequently validated against experimental data at different operating conditions, and was then used in optimisation studies to determine optimal operating conditions.

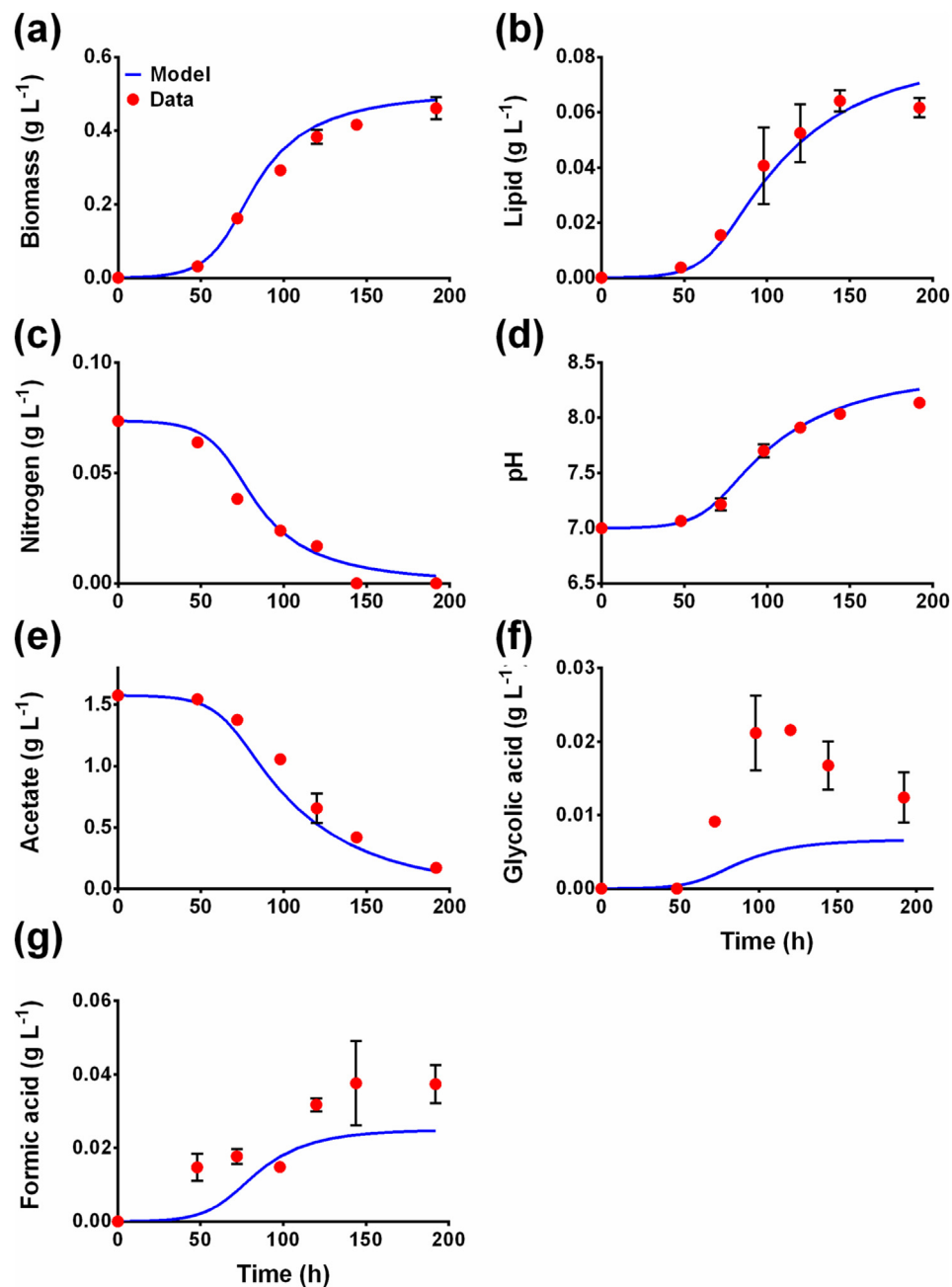


**Fig. 3.** Validation of model predictions (lines) by experimental data (symbols with error bars) for: (a) biomass, (b) lipid concentration, (c) substrate (acetate) consumption, (d) N consumption, (e) pH change, (f) oxalic acid production, (g) glycolic acid production and (h) formic acid production, using  $1.575 \text{ g L}^{-1}$  acetate and  $0.0735 \text{ g L}^{-1}$  N.

#### 4.1. Experimental results

Measurements of microalgal growth, as determined by biomass concentration, and lipid accumulation (Fig. 1 and Fig. S1) were taken alongside measurements of growth media pH change and organic acid concentrations, for the six different acetate concentrations and the seven different N concentrations mentioned in Section 2.1, in order to examine the effect of the change in nutrient and substrate concentration on the overall biomass and lipid concentrations. For the acetate-absent and acetate-deficient ( $0 \text{ g L}^{-1}$  and  $0.42 \text{ g L}^{-1}$ ) as well as the acetate-excess ( $4.2 \text{ g L}^{-1}$ ) media, dry biomass was below detectable levels for the first 120 h due to slow growth rate (Fig. S1a). Thus lipid concentration was also undetectable (Fig. S1b). Cells grown in the other acetate concentrations ( $1.05 \text{ g L}^{-1}$ ,  $2.1 \text{ g L}^{-1}$  and  $3.15 \text{ g L}^{-1}$ ) grew rapidly with equivalent growth profiles. Compared to the  $1.05 \text{ g L}^{-1}$  acetate

treatment, biomass concentration decreased significantly ( $p < 0.0001$ , one-way ANOVA) both for the acetate excess ( $4.2 \text{ g L}^{-1}$ ) treatment, by approximately 50%, and for the acetate-deficient ( $0.42 \text{ g L}^{-1}$ ) and absent ( $0 \text{ g L}^{-1}$ ) treatments, by approximately 80% (Fig. 1a). In contrast, biomass concentration was essentially the same for the  $1.05 \text{ g L}^{-1}$ ,  $2.1 \text{ g L}^{-1}$  and  $3.15 \text{ g L}^{-1}$  acetate treatments. Many chlorophyte microalgae species such as *C. reinhardtii* are able to efficiently grow heterotrophically and this is increasingly being considered as a more commercially viable method of high-productive cultivation [38]. While organic carbon addition such as acetate can indeed increase biomass concentration, as we show here, the inhibition of growth by excessive concentrations of acetate may either be due to acetate toxicity or a saturation of acetate assimilation and metabolism, coupled to the acetate-induced inhibition of photosynthesis [14,34]. Acetate is metabolised via the glyoxylate cycle, but can also be converted into acetyl-CoA in an

ATP-dependent mechanism and then used as a substrate for fatty acid synthesis and then TAG metabolism [34]. Increase in lipid concentration as acetate concentration increases might therefore be predicted and indeed this has been previously observed in *C. reinhardtii* under both N sufficient and N limited conditions [44]. However, we found that the proportion of lipid accumulation within the cell on a total dry weight basis was essentially identical for all acetate treatments (approximately 10% lipid), and therefore the difference in volumetric lipid concentration between the treatments (Fig. 1b) was almost entirely due to the difference in biomass. This therefore suggests that under these N sufficient ( $0.098 \text{ g L}^{-1} \text{ N}$ ) conditions, assimilated acetate is being used predominantly for cell growth. It is also worth noting that the study of Ramanan et al. [44] evaluated acetate addition in a mutant strain of *C. reinhardtii* that was unable to produce starch, whereas in wild type strains acetate addition has been suggested to drive carbon allocation preferentially towards starch accumulation rather than lipid [14].

For the N deficient ( $0.0049 \text{ g L}^{-1}$  and  $0.0098 \text{ g L}^{-1}$ ) and N excess ( $0.98 \text{ g L}^{-1}$  and  $1.96 \text{ g L}^{-1}$ ) media, dry biomass concentration (and therefore lipid concentration) was again below level of detection for the first 120 h due to slow growth rate (Fig. S1c and d). As expected for an essential nutrient, and in agreement with previous studies, N limitation significantly inhibited growth compared to the  $0.098 \text{ g L}^{-1} \text{ N}$  replete treatment ( $p < 0.0001$  for  $0.0049 \text{ g L}^{-1}$  and  $0.0098 \text{ g L}^{-1} \text{ N}$ ;  $p = 0.0009$  for  $0.049 \text{ g L}^{-1} \text{ N}$ , one-way ANOVA), with the lowest biomass concentration ( $0.149 \text{ g L}^{-1}$ ) seen for the  $0.0049 \text{ g L}^{-1} \text{ N}$  concentration (Fig. 1c). However, the highest N concentrations ( $0.98 \text{ g L}^{-1}$  and  $1.96 \text{ g L}^{-1}$ ) also significantly inhibited growth ( $p < 0.0001$ , one-way ANOVA), possibly due to partial toxicity when ammonium concentration is too high (Fig. 1c). As anticipated, N limitation led to an increase in lipid accumulation compared to the higher N concentrations, with the  $0.049$ ,  $0.0098$  and  $0.0049 \text{ g L}^{-1} \text{ N}$  treatments inducing cellular (per dry weight) lipid content values of 15.6%, 21.8% and 26%,

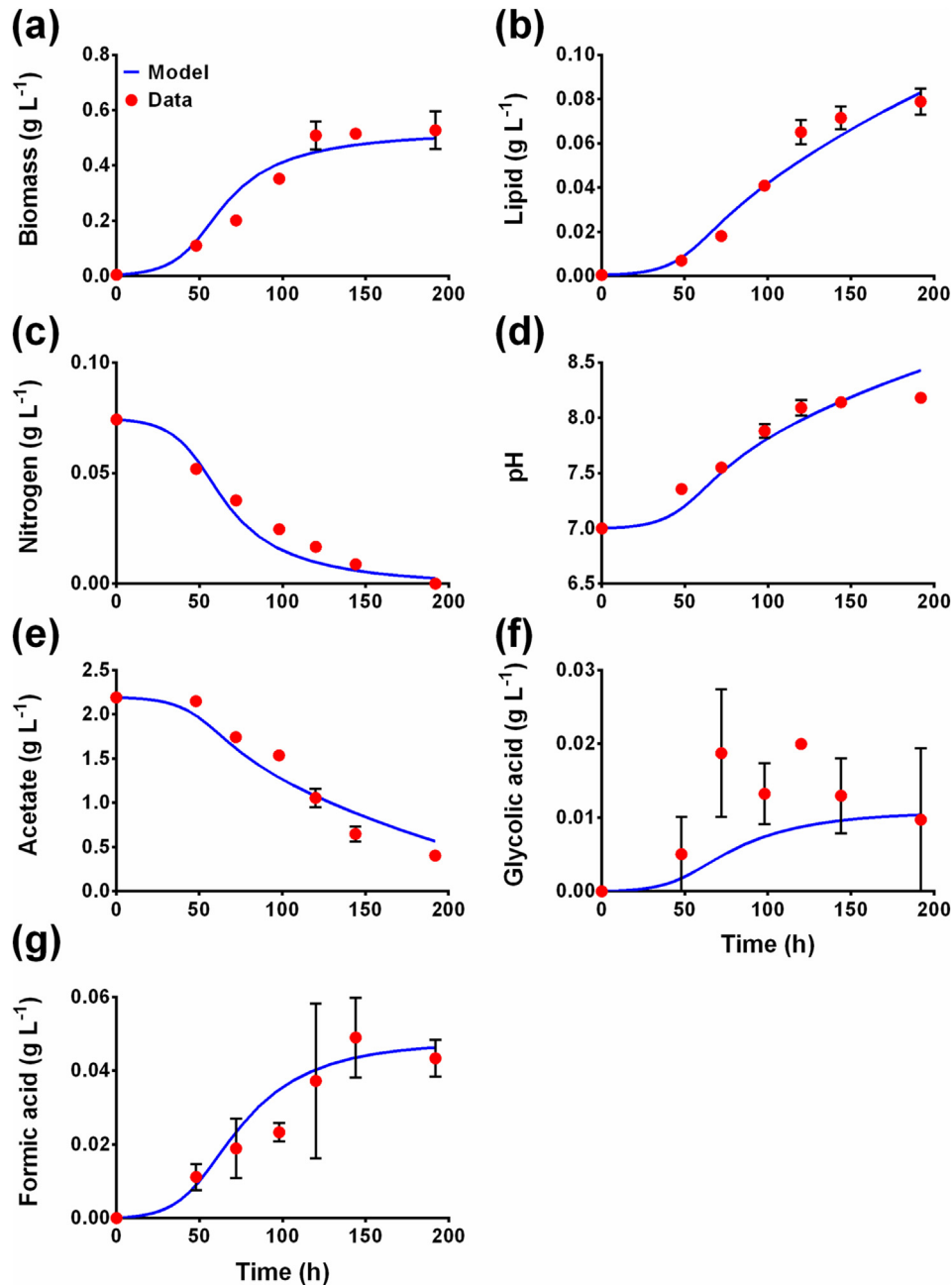


Fig. 4. Optimization of model predictions (lines) by experimental data (symbols with error bars) for: (a) biomass, (b) lipid concentration, (c) substrate (acetate) consumption, (d) N consumption, (e) pH change, (f) oxalic acid production, (g) glycolic acid production and (h) formic acid production, using  $2.1906 \text{ g L}^{-1}$  acetate and  $0.0742 \text{ g L}^{-1} \text{ N}$ .



**Table 2**  
Optimal system initial conditions and resulted productivity and yield measures.

Initial conditions	Base case runs		Optimisation runs	
Biomass concentration		0.001 g L <sup>-1</sup>		0.005 g L <sup>-1</sup>
Acetate concentration		2.1 g L <sup>-1</sup>		2.1906 g L <sup>-1</sup>
Nitrogen concentration		0.098 g L <sup>-1</sup>		0.0742 g L <sup>-1</sup>
Resulted measures	Base case Results	Optimized results	Change	Experimental results
Lipid concentration	62.4 mg L <sup>-1</sup>	82.9 mg L <sup>-1</sup>	+20.5 mg L <sup>-1</sup>	84.7 mg L <sup>-1</sup>
Lipid productivity	7.8 mg L <sup>-1</sup> d <sup>-1</sup>	10.3625 mg L <sup>-1</sup> d <sup>-1</sup>	+32.85%	10.5875 mg L <sup>-1</sup> d <sup>-1</sup>
Biomass concentration	586.8 mg L <sup>-1</sup>	498.4 mg L <sup>-1</sup>	-88.4 mg L <sup>-1</sup>	458.6 mg L <sup>-1</sup>
Biomass productivity	73.85 mg L <sup>-1</sup> d <sup>-1</sup>	62.3 mg L <sup>-1</sup> d <sup>-1</sup>	-15.65%	57.325 mg L <sup>-1</sup> d <sup>-1</sup>

respectively, compared to 9 to 10% lipid content in the N replete (0.098 g L<sup>-1</sup>) cells. This is in agreement with many previous N limitation studies where substantial lipid induction can be observed as N availability becomes starved [5]. N excess did not inhibit cellular lipid accumulation but on a volumetric basis, lipid concentration was lowest with 0.98 g L<sup>-1</sup> and 1.96 g L<sup>-1</sup> N (0.261 g L<sup>-1</sup>, 0.221 g L<sup>-1</sup> respectively) and highest with 0.049 g L<sup>-1</sup> and 0.098 g L<sup>-1</sup> N (0.3645 g L<sup>-1</sup>, 0.5335 g L<sup>-1</sup> respectively) (Fig. 1d), with the low lipid yield at the highest N concentrations explained by the reduced biomass at these concentrations (Fig. 1c).

#### 4.2. Model validation

We have subsequently carried out a validation study for our constructed model to assess its predictive capabilities. In Fig. 3, the model predictions for the experimental results, obtained at base line conditions (1.5735 g L<sup>-1</sup> acetate, 0.0735 g L<sup>-1</sup> N, 1 mg L<sup>-1</sup> biomass, and pH 7, and with starting organic acid (GA and FA) by-product concentrations all at 0 g L<sup>-1</sup>) are presented. The system was operated at room temperature  $T = 25$  °C and the light illumination ( $I_0$ ) is considered constant and equal to 125  $\mu\text{Em}^{-2}\text{s}^{-1}$ . The model was capable of predicting the experimentally obtained concentrations of biomass, lipid, acetate, N, and the pH change with high precision as well as the concentrations of organic acid by-products with reasonable accuracy (Error = 2.9819). Thus, the detailed multiplicative model proposed in this study can be used for precise prediction of the dynamic behaviour of bench-scale batch experiments.

#### 4.3. Process optimization

The validated model was further exploited in an optimization study to determine the optimal operating conditions for such bench-scale systems. Here, the optimization problem was set up to calculate the maximum lipid and biomass productivities:

$$\text{Objective} = \max(J_L + J_X) \quad \text{Eq. 13}$$

subject to the governing system equations (Eqs. 5 to 11). The productivities are defined as:

$$J_L = \frac{L - L_0}{t_p - t_{p_0}} \quad \text{Eq. 14}$$

$$J_X = \frac{X - X_0}{t_p - t_{p_0}} \quad \text{Eq. 15}$$

where  $J_L$  is the productivity of lipid (mg L<sup>-1</sup>s<sup>-1</sup>),  $J_X$  is the productivity of biomass (mg L<sup>-1</sup>s<sup>-1</sup>),  $L$  is the final lipid concentration (mg Lipid L<sup>-1</sup>) calculated by Eq. 6,  $L_0$  is the initial lipid concentration (mg Lipid L<sup>-1</sup>),

$t_p$  is the process time (h),  $X$  is the final biomass concentration (mg Biomass L<sup>-1</sup>) calculated by Eq. 5 and  $X_0$  is the initial biomass concentration (mg Biomass L<sup>-1</sup>).

The substrate, nitrogen and inoculum initial concentrations were the degrees of freedom in the optimization process. The computed optimum is tabulated in Table 2. Optimum lipid productivity is achieved using initial concentrations of acetate, N and inoculum equal to 2.1906 g L<sup>-1</sup>, 0.0742 g L<sup>-1</sup> and 0.005 g L<sup>-1</sup>, respectively. This represents a 32.85% increase in the lipid oil productivity compared to the base case, which illustrates the effectiveness of computer-based optimisation for such systems. The optimization results were experimentally validated. The computed optimal dynamics along with the corresponding experimental results obtained at the optimal operating conditions are presented in Fig. 4. The agreement between the computed and experimental results is very good (error = 2.6249), which illustrates the usefulness of our model for optimal design of experiments, minimizing the need of time-consuming and potentially expensive trial-and-error runs [1,25,37].

## 5. Conclusions

Few studies have attempted to model microalgal biomass growth and lipid accumulation but none of these previously developed models have considered the simultaneous and antagonistic effect of nutrient starvation, substrate concentration and light intensity on the rate of lipid production and rate of biomass growth. Consequently, these models do not allow the accurate analysis of the culture system behaviour under different operating conditions. A multi-parameter model was developed in this study to predict the dynamic behaviour of all 7 system state variables accurately, by considering the effect of three different culture variables (S, N, I). Experimental studies were conducted for the investigation of the effect of varying substrate (acetate) and nutrient (N) on biomass growth and on lipid accumulation rates, and used in conjunction with the constructed model for the estimation of kinetic parameters that are essential for accurate system simulations. The model was validated for a different set of initial concentrations. Optimization of the process was carried out to determine the optimal system operating conditions and it was found that a 32.85% increase in the lipid oil productivity was achieved using 2.1906 g L<sup>-1</sup> acetate, 0.0742 g L<sup>-1</sup> N and 0.005 g L<sup>-1</sup> starting biomass inoculum. This illustrates the usefulness not only of computer-based optimisation studies for the improvement of microalgal-based production, but also of carefully constructed predictive models for the accurate simulation of these systems. Such predictive models can be exploited for the robust design, control and scale-up of microalgal oil production, which can help to bring this important technology closer to commercialization and industrial applicability.

## Acknowledgements

MB would like to acknowledge the financial support of the Republic of Turkey Ministry of National Education. ISF wishes to acknowledge the Engineering and Physical Sciences Research Council for its financial support through his EPSRC doctoral prize fellowship 2014.

## Appendix A. Supplementary data

Supplementary data to this article can be found online at <http://dx.doi.org/10.1016/j.algal.2016.12.015>.

## References

- [1] V.O. Adesanya, M.P. Davey, S.A. Scott, A.G. Smith, Kinetic modelling of growth and storage molecule production in microalgae under mixotrophic and autotrophic conditions, *Bioresour. Technol.* 157 (2014) 293–304.
- [2] A.L. Ahmad, N.H.M. Yasin, C.J.C. Derek, J.K. Lim, Microalgae as a sustainable energy source for biodiesel production: a review, *Renew. Sust. Energ. Rev.* 15 (2011) 584–593.
- [3] S. Aiba, Growth kinetics of photosynthetic microorganisms, *Microbial Reactions*, Springer Berlin Heidelberg, Berlin, Heidelberg, 1982.
- [4] J.F. Andrews, A mathematical model for the continuous culture of microorganisms utilizing inhibitory substrates, *Biotechnol. Bioeng.* 10 (1968) 707–723.
- [5] A.K. Bajhaiya, A.P. Dean, T. Driver, D.K. Trivedi, N.J.W. Rattray, J.W. Allwood, R. Goodacre, J.K. Pittman, High-throughput metabolic screening of microalgae genetic variation in response to nutrient limitation, *Metabolomics* 12 (2016) 1–14.
- [6] Q. Béchet, A. Shilton, B. Guieysse, Modeling the effects of light and temperature on algae growth: state of the art and critical assessment for productivity prediction during outdoor cultivation, *Biotechnol. Adv.* 31 (2013) 1648–1663.
- [7] M. Bekirogullari, J. Pittman, C. Theodoropoulos, Integrated computational and experimental studies of microalgal production of fuels and chemicals, in: K.V. Gernaey, K.H. J., G. Rafiqul (Eds.), *Computer Aided Chemical Engineering*, Elsevier, 2015.
- [8] O. Bernard, Hurdles and challenges for modelling and control of microalgae for CO<sub>2</sub> mitigation and biofuel production, *J. Process Control* 21 (2011) 1378–1389.
- [9] O. Bernard, F. Mairet, B. Chachuat, Modelling of Microalgae Culture Systems with Applications to Control and Optimization, in: C. Posten, S. Feng Chen (Eds.), *Microalgae Biotechnology*, Cham, Springer International Publishing, 2016.
- [10] O. Bernard, B. Rémond, Validation of a simple model accounting for light and temperature effect on microalgal growth, *Bioresour. Technol.* 123 (2012) 520–527.
- [11] M.A. Borowitzka, Commercial production of microalgae: ponds, tanks, tubes and fermenters, *J. Biotechnol.* 70 (1999) 313–321.
- [12] L. Brennan, P. Owende, Biofuels from microalgae—a review of technologies for production, processing, and extractions of biofuels and co-products, *Renew. Sust. Energ. Rev.* 14 (2010) 557–577.
- [13] G. Breuer, P.P. Lamers, M. Janssen, R.H. Wijffels, D.E. Martens, Opportunities to improve the areal oil productivity of microalgae, *Bioresour. Technol.* 186 (2015) 294–302.
- [14] S.P. Chapman, C.M. Paget, G.N. Johnson, J.-M. Schwartz, Flux balance analysis reveals acetate metabolism modulates cyclic electron flow and alternative glycolytic pathways in *Chlamydomonas reinhardtii*, *Front. Plant Sci.* 6 (2015) 474.
- [15] F. Chen, M.R. Johns, Substrate inhibition of *Chlamydomonas reinhardtii* by acetate in heterotrophic culture, *Process Biochem.* 29 (1994) 245–252.
- [16] F. Chen, M.R. Johns, Heterotrophic growth of *Chlamydomonas reinhardtii* on acetate in chemostat culture, *Process Biochem.* 31 (1996) 601–604.
- [17] L. Chiari, A. Zecca, Constraints of fossil fuels depletion on global warming projections, *Energ Policy* 39 (2011) 5026–5034.
- [18] Y. Chisti, Biodiesel from microalgae, *Biotechnol. Adv.* 25 (2007) 294–306.
- [19] A. Converti, A.A. Casazza, E.Y. Ortiz, P. Perego, M. Del Borghi, Effect of temperature and nitrogen concentration on the growth and lipid content of *Nannochloropsis oculata* and *Chlorella vulgaris* for biodiesel production, *Chem. Eng. Process. Process Intensif.* 48 (2009) 1146–1151.
- [20] A. Demirbas, M. Fatih Demirbas, Importance of algae oil as a source of biodiesel, *Energ Convers. Manag.* 52 (2011) 163–170.
- [21] G. Dragone, B.D. Fernandes, A.A. Vicente, J.A. Teixeira, Third Generation Biofuels from Microalgae, 2010.
- [22] T. Driver, A. Bajhaiya, J.K. Pittman, Potential of bioenergy production from microalgae, *Current Sustainable/Renewable Energy Reports* 1 (2014) 94–103.
- [23] C.N. Economou, G. Aggelis, S. Pavlou, D.V. Vayenas, Modeling of single-cell oil production under nitrogen-limited and substrate inhibition conditions, *Biotechnol. Bioeng.* 108 (2011) 1049–1055.
- [24] R.A. Efrogmson, V.H. Dale, Environmental indicators for sustainable production of algal biofuels, *Ecol. Indic.* 49 (2015) 1–13.
- [25] S. Fouchard, J. Pruvost, B. Degrenne, M. Titica, J. Legrand, Kinetic modeling of light limitation and sulfur deprivation effects in the induction of hydrogen production with *Chlamydomonas reinhardtii*: part I. Model development and parameter identification, *Biotechnol. Bioeng.* 102 (2009) 232–245.
- [26] D.R. Georgianna, S.P. Mayfield, Exploiting diversity and synthetic biology for the production of algal biofuels, *Nature* 488 (2012) 329–335.
- [27] E.C. Goncalves, A.C. Wilkie, M. Kirst, B. Rathinasabapathi, Metabolic regulation of triacylglycerol accumulation in the green algae: identification of potential targets for engineering to improve oil yield, *Plant Biotechnology Journal*, n/a-n/a. (2015).
- [28] M.J. Griffiths, S.T.L. Harrison, Lipid productivity as a key characteristic for choosing algal species for biodiesel production, *J. Appl. Phycol.* 21 (2009) 493–507.
- [29] E.M. Grima, F.G. Camacho, J.A.S. Pérez, J.M.F. Sevilla, F.G.A. Fernández, A.C. Gómez, A mathematical model of microalgal growth in light-limited chemostat culture, *J. Chem. Technol. Biotechnol.* 61 (1994) 167–173.
- [30] E.H. Harris, *The Chlamydomonas Sourcebook: A Comprehensive Guide to Biology and Laboratory Use*, Academic Press, Inc., San Diego, 1989.
- [31] M. Hoel, S. Kverndokk, Depletion of fossil fuels and the impacts of global warming, *Resour. Energy Econ.* 18 (1996) 115–136.
- [32] G.O. James, C.H. Hocart, W. Hillier, H. Chen, F. Kordbacheh, G.D. Price, M.A. Djordjevic, Fatty acid profiling of *Chlamydomonas reinhardtii* under nitrogen deprivation, *Bioresour. Technol.* 102 (2011) 3343–3351.
- [33] Y.-C. Jeon, C.-W. Cho, Y.-S. Yun, Measurement of microalgal photosynthetic activity depending on light intensity and quality, *Biochem. Eng. J.* 27 (2005) 127–131.
- [34] X. Johnson, J. Alric, Central carbon metabolism and electron transport in *Chlamydomonas reinhardtii*: metabolic constraints for carbon partitioning between oil and starch, *Eukaryotic cell* 12 (2013) 776–793.
- [35] S.E. Jørgensen, A eutrophication model for a lake, *Ecol. Model.* 2 (1976) 147–165.
- [36] K. Kovárová-Kovar, T. Egli, Growth kinetics of suspended microbial cells: from single-substrate-controlled growth to mixed-substrate kinetics, *Microbiol. Mol. Biol. Rev.* 62 (1998) 646–666.
- [37] E. Lee, M. Jalalizadeh, Q. Zhang, Growth kinetic models for microalgae cultivation: a review, *Algal Res.* 12 (2015) 497–512.
- [38] J. Lowrey, R.E. Armenta, M.S. Brooks, Nutrient and media recycling in heterotrophic microalgae cultures, *Appl. Microbiol. Biotechnol.* 100 (2016) 1061–1075.
- [39] R. Miller, G. Wu, R.R. Deshpande, A. Vieler, K. Gärtner, X. Li, E.R. Moellering, S. Zäuner, A.J. Cornish, B. Liu, Changes in transcript abundance in *Chlamydomonas reinhardtii* following nitrogen deprivation predict diversion of metabolism, *Plant Physiol.* 154 (2010) 1737–1752.
- [40] J. Monod, The growth of bacterial cultures, *Annu. Rev. Microbiol.* 3 (1949) 371–394.
- [41] J. O'grady, J.A. Morgan, Heterotrophic growth and lipid production of *Chlorella protothecoides* on glycerol, *Bioprocess Biosyst. Eng.* 34 (2010) 121–125.
- [42] J.C. Ogonna, H. Yada, H. Tanaka, Kinetic study on light-limited batch cultivation of photosynthetic cells, *J. Ferment. Bioeng.* 80 (1995) 259–264.
- [43] J.K. Pittman, A.P. Dean, O. Osundeko, The potential of sustainable algal biofuel production using wastewater resources, *Bioresour. Technol.* 102 (2011) 17–25.
- [44] R. Ramanan, B.-H. Kim, D.-H. Cho, S.-R. Ko, H.-M. Oh, H.-S. Kim, Lipid droplet synthesis is limited by acetate availability in starchless mutant of *Chlamydomonas reinhardtii*, *FEBS Lett.* 587 (2013) 370–377.
- [45] M. Siaux, S. Cuiñé, C. Cagnon, B. Fessler, M. Nguyen, P. Carrier, A. Beyly, F. Beisson, C. Triantaphyllidis, Y. Li-Beisson, G. Peltier, Oil accumulation in the model green alga *Chlamydomonas reinhardtii*: characterization, variability between common laboratory strains and relationship with starch reserves, *BMC Biotechnol.* 11 (2011) 1–15.
- [46] E. Spijkerman, F. De Castro, U. Gaedke, Independent colimitation for carbon dioxide and inorganic phosphorus, *PLoS One* 6 (2011), e28219.
- [47] R. Tevatia, Y. Demirel, P. Blum, Kinetic modeling of photoautotrophic growth and neutral lipid accumulation in terms of ammonium concentration in *Chlamydomonas reinhardtii*, *Bioresour. Technol.* 119 (2012) 419–424.
- [48] A. Vlysidis, M. Binns, C. Webb, C. Theodoropoulos, Glycerol utilisation for the production of chemicals: conversion to succinic acid, a combined experimental and computational study, *Biochem. Eng. J.* 58–59 (2011) 1–11.
- [49] D. Zhang, P. Dechatiwongse, E.A. Del Rio-Chanona, G.C. Maitland, K. Hellgardt, V.S. Vassiliadis, Modelling of light and temperature influences on cyanobacterial growth and biohydrogen production, *Algal Res.* 9 (2015) 263–274.
- [50] X.-W. Zhang, F. Chen, M.R. Johns, Kinetic models for heterotrophic growth of *Chlamydomonas reinhardtii* in batch and fed-batch cultures, *Process Biochem.* 35 (1999) 385–389.
- [51] M. Allen, Excretion of organic compounds by *Chlamydomonas*, *Arch. Mikrobiol.* 24 (1956) 163–168.
- [52] J. McNichol, K. Macdougall, J. Melanson, P. McGinn, Suitability of Soxhlet Extraction to Quantify Microalgal Fatty Acids as Determined by Comparison with In Situ Transesterification, *Lipids* 47 (2012) 195–207.